

# Internal to external wavelength calibration

---

Kailash C. Sahu  
Jan 13, 1999

---

## ABSTRACT

*The spectra of Hen 1357 (the Stingray nebula) were used to check the internal to external wavelength calibration of the STIS first order CCD modes. The radial velocity of the Stingray nebula is known to high accuracy ( $< 1$  km/sec) and the line width of the nebular line is very narrow ( $< 8$  km/sec for the integrated nebula). Thus the observations of the Stingray nebula are ideal to check the internal to external wavelength calibration of the first order modes. The observations were taken in G430L and G750M modes using a  $52 \times 0.05$  arcsec slit covering the wavelength range 2900 to 5700 Å and 6295 to 6867 Å, respectively. The observed wavelength range includes many nebular emission lines. The wavelengths of the nebular lines derived using the pipeline internal wavelength calibration were compared with the wavelengths derived from other ground based observations. In all cases, the wavelength match between the two is of the same order as the accuracy to which the line center can be measured. These results imply that there is no significant offset between the internal and external wavelength calibrations for these modes. The HDF-S QSO observations were also used for this test both for the first order and the Echelle modes. The results of the HDF-S QSO observations further confirm the above finding for the first order modes, and imply that there is no significant offset between the internal and external wavelength calibration for the Echelle modes.*

---

## 1. Introduction

The optical path for the CCD spectroscopic modes is slightly different for an external target and the internal lamps (Woodgate et al. 1998). Although the slightly different optical paths are not expected to give rise to a shift in the wavelength calibration for internal and external targets, it is important to verify know that this, and check that there is no unexpected factor causing an undesired wavelength shift. The calibration observations of the Stingray nebula, as explained below, are ideal to carry out this test. The observations of the Stingray nebula were used to obtain an estimate of the offset between the internal and

external wavelength calibrations of several CCD first order modes. In addition, the recent HDF-south observations, taken for the first order CCD and MAMA, and Echelle MAMA modes, were also used to verify the internal to external wavelength calibrations.

## **2. The Stingray Nebula**

The Stingray nebula (or Hen 1357) was first detected as a proto-planetary nebula candidate in a program designed to pick out protoplanetary nebulae from their IRAS-infrared colors (Waters and Sahu, 1988). Hen 1357 was classified as a B-type star with H-alpha emission, with no other emission line present in its spectrum taken in 1970. However, a spectrum of this source, taken in 1991 by Sahu with the ESO 1.5 m telescope and the Bolter and Chivens spectrograph, showed an abundance of emission lines, characteristic of planetary nebulae (Parthasarathy et al. 1988). Hen 1357 was then observed with the high-resolution spectrograph at the ESO 1.4m Coude-Auxilliary telescope, with a resolving power of 100,000. The emission lines were found to be uncharacteristically narrow, less than about 8 km/sec FWHM. The source was spatially unresolved from the ground, suggesting that the total extent of the nebula is less than 2 arcsec. The observed radial velocity of the source is 13 km/s.

An HST image of the nebula (Bobrowsky et al. 1998) shows that this is now a bonafide planetary nebula, and the extent of the nebula is currently about 1.6 arcsec. The nebula is now named the 'Stingray' because of its appearance). It has strong emission lines, the emission lines are narrow, and its radial velocity is known to high accuracy. This makes it an ideal target to check the internal to external wavelength calibration of the STIS first order modes.

## **3. HDF-South observations**

The QSO in the HDF-south is a relatively bright target, which was observed with the STIS G430M, G140L, G140M, G230L and E230M modes (Williams et al. 1999). The wavelength calibration for these observations were carefully carried out using the internal calibration lamp spectra. Ground based high-resolution spectra of this QSO exist, with some overlapping regions. Thus the observations of the HDF-S QSO provide a second dataset on which to check the internal to external wavelength calibration both for the first order CCD and MAMA modes and the Echelle modes. This ISR also reports the results obtained from this test.

**Table 1.** Details of the observations of the Stingray Nebula

Grating	Slit	Cenwave (A)	Wavelength range (A)	Disp (A/pix)	Texp (sec)
G750M	52 x 0.05	6581	6295 - 6867	0.56	700
G430L	52 x 0.05	4300	2900 - 5700	2.73	700

#### 4. Observations:

Observations of the Stingray nebula were taken in G750M and G430L modes, the details of which are given in Table 1. Observations of the QSO in the HDF-S were taken with the G430M, G230L, E230M and G140L gratings, the details of which are given in Table 2.

**Table 2.** Details of the STIS spectroscopic observations of the HDF-S QSO

Grating	Slit	Cenwave (A)	Wavelength range (A)	Disp (A/pix)	Texp (sec)
G430M	52 x 0.2	3165, 3423	3025 - 3565	0.28	54,892
G230L	52 x 0.2	2376	2200 - 2900	1.58	18,424
E230M	0.2 x 0.2	2707	2300 - 3100	~1.5 to 4	151,074
G140L	52 x 0.2	1425	1167 - 1590	0.6	18,480

#### 5. Analysis

The observations of the Stingray nebula were wavelength calibrated via standard procedures in calstis, using contemporaneous observations of the internal calibration lamp. The latest weekly dark frames were used and the pipeline calibration of the dataset was carried out using calstis. Since the object is clearly extended, x1d step was omitted. For Doppler correction due to the motion of the spacecraft, the x,y,z components (VELOC-STX, etc) spacecraft motion were taken from the \_spt files. The dot-product of this vector with the rectangular coordinates of the source was used to estimate the Doppler correction. The calculated Doppler correction is about 0.4 km/sec, which is less than 0.1 pixels even in the higher dispersion G750M mode, and was ignored in further analysis.

The G750M (cenwave=6581A) observations cover the wavelength range 6295 to 6867 A. This included three strong emission lines in the spectrum: the H $\alpha$  6563 A line, and the [NII] doublet at 6548 and 6584 A. (Note that the wavelengths noted here refer to the com-

monly used air-wavelengths, which have been converted to vacuum-wavelengths in the Tables 3 and 4).

The G430L spectra covered the wavelength region 2900 Å to 5700 Å which include several strong emission lines, the strongest of them (which are used for the analyses here) being H $\beta$  4861 Å, and the [OIII] doublet at 4959 Å and 5007 Å (air-wavelengths!).

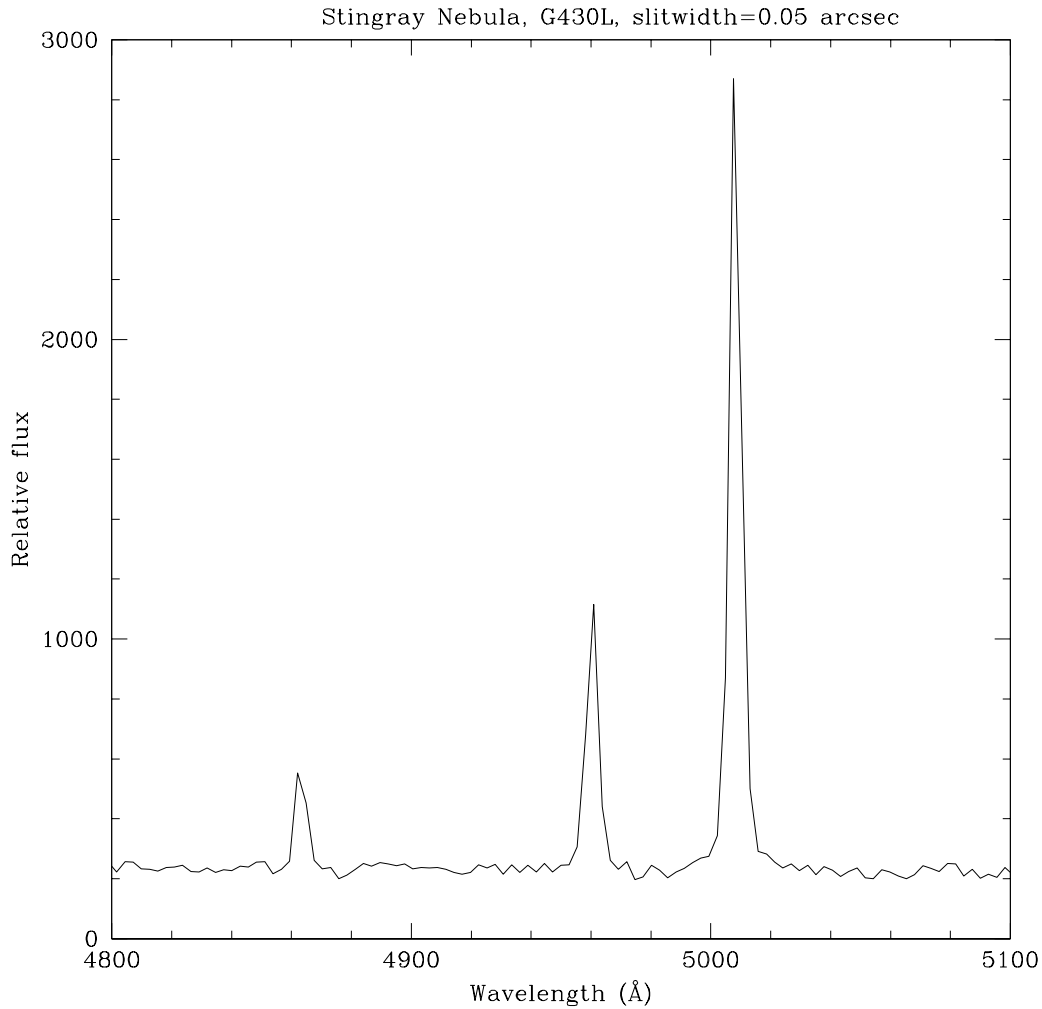


**Fig. 1.** G430L spectrum of the Stingray nebula.

Since the source is extended, it is important to check whether there is any shift in the line center at different positions along the slit. The line center is fixed within 0.1 pixels at various positions along the slit, as expected from the fact that the width of the emission line is about 8 km/sec.

## 6. Results

The line centers of different emission lines were determined by fitting gaussians to the lines using 'splot'. Example fits are shown in Fig. 1 and Fig. 2 for G750M and G430L observations, respectively. The derived line centers, along with the line centers derived from ground-based high-resolution observations are given in Table 3.

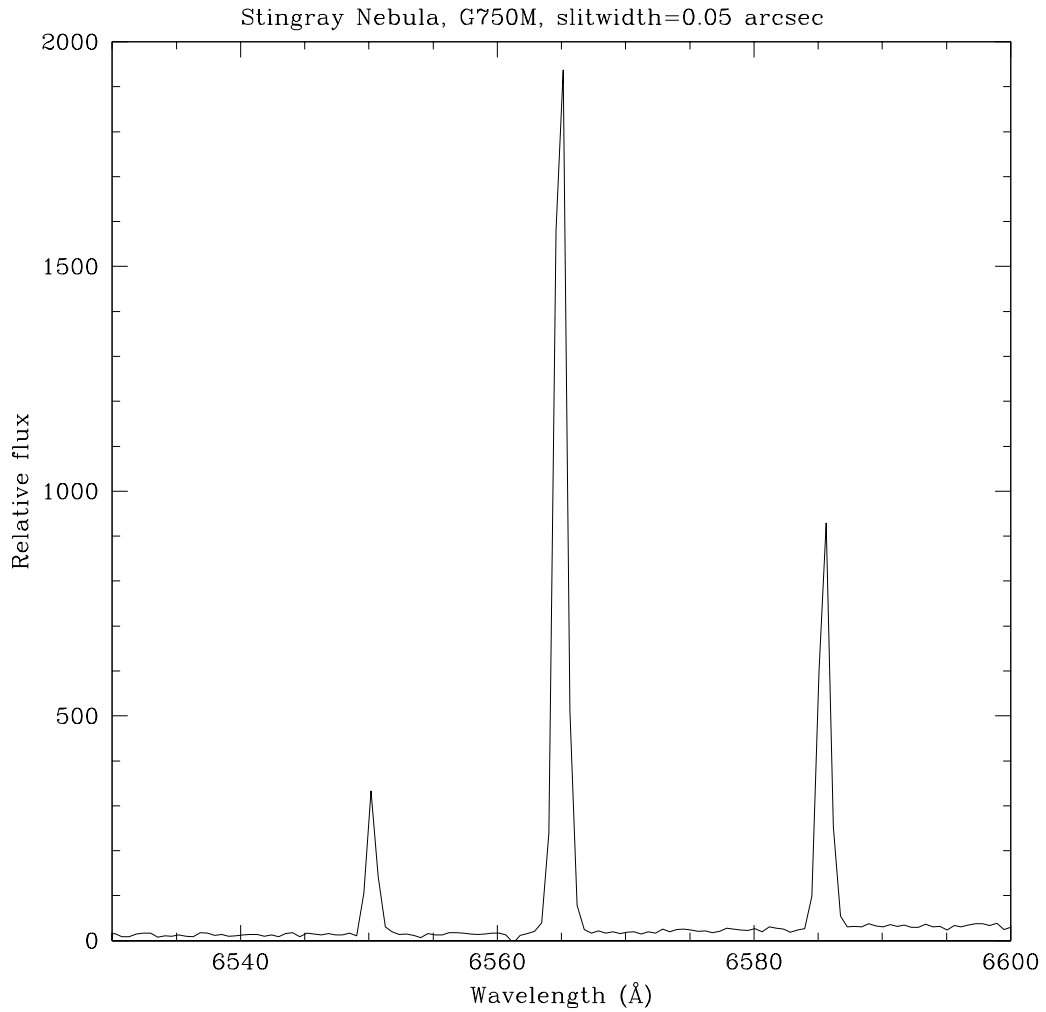


**Fig. 2.** G750M spectrum of the Stingray nebula.

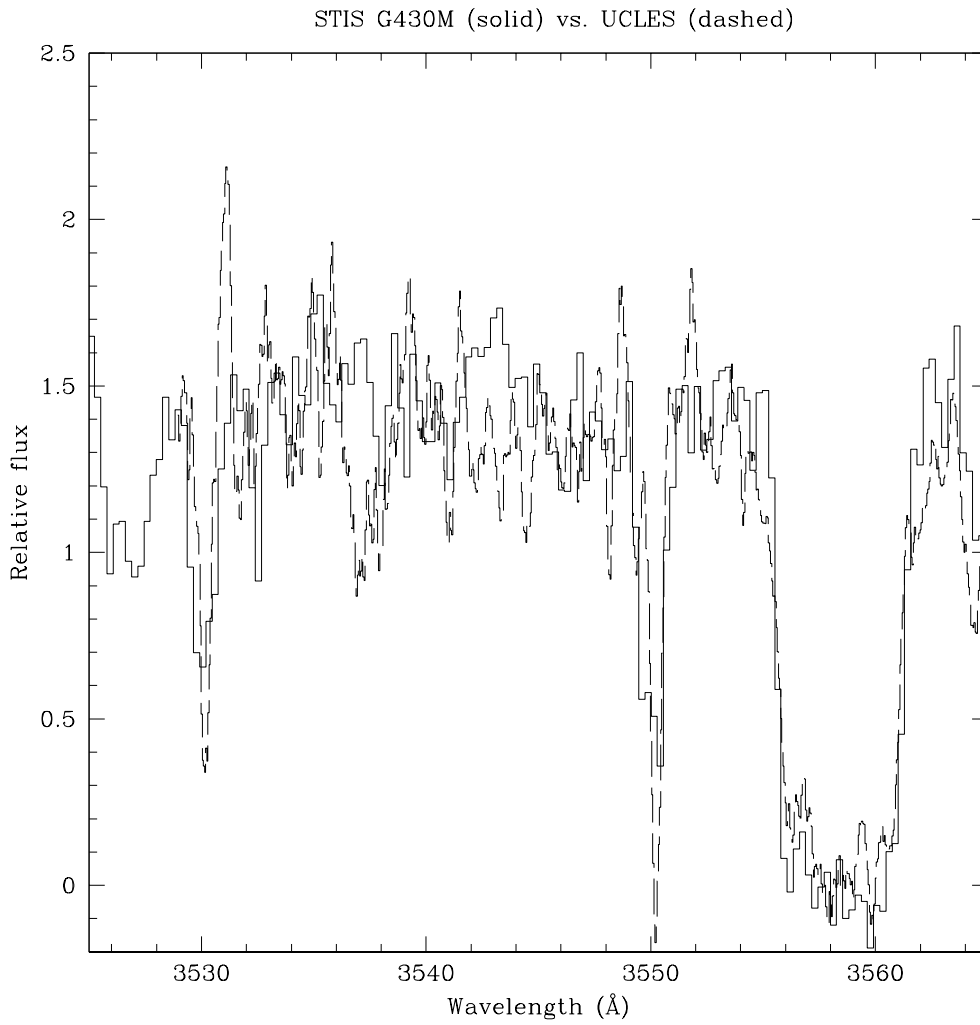


**Fig. 3.** Comparison of STIS G430M data (solid) with UCLES data (dashed).

**Table 3.** Observed line centers\* and comparison with other observations in G750M mode

Line ID (I)	$\lambda_{\text{rest}}$ (Å) (II)	$\lambda_{\text{obs}}$ (Å) (III)	$\lambda_{\text{exp}}$ (Å) (IV)	Diff (Å) (III - IV)
[NII]	6549.93	6550.26	6550.21	0.05
H $\alpha$	6564.64	6564.84	6564.92	-0.08
[NII]	6585.24	6585.49	6585.52	-0.03

\*All the wavelengths in the Table refer to vacuum wavelengths.

The accuracy in the determination of the line center is typically 1/10 of a pixel, which corresponds to 0.06 Å and 0.27 Å for the G750M and G430L gratings, respectively. The difference between the observed and the expected wavelengths is of the same order as the accuracy to which the line centers can be determined. This shows that, to within the observational accuracy, there is no offset between the internal and external wavelength calibrations in the STIS first order modes.

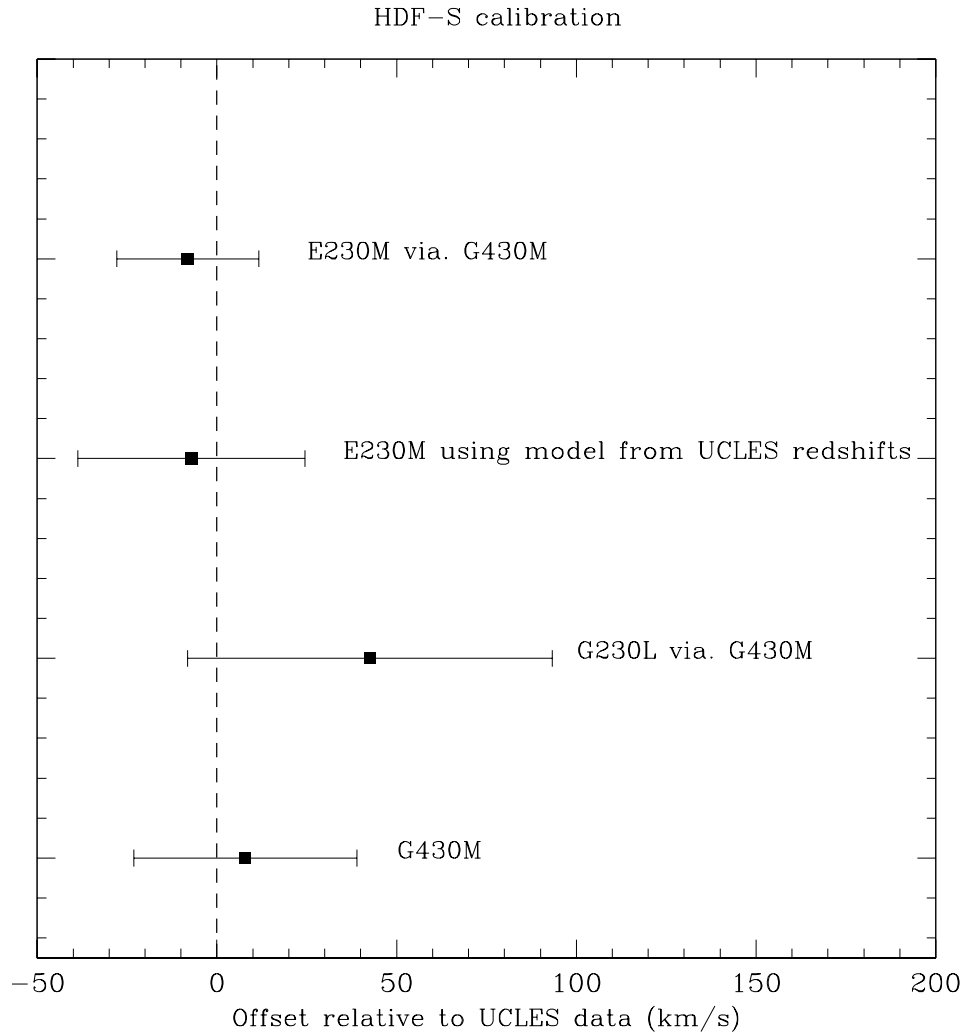
**Table 4.** Observed line centers and comparison with other observations in G430L mode

Line ID (I)	$\lambda_{\text{rest}}$ (Å) (II)	$\lambda_{\text{obs}}$ (Å) (III)	$\lambda_{\text{exp}}$ (Å) (IV)	Diff (Å) (III - IV)
H $\beta$	4862.74	4862.36	4862.95	0.11
[OIII]	4960.29	4960.31	4960.50	-0.21
[OIII]	5008.30	5008.19	5008.51	-0.32

## 7. HDF-S QSO observations

The HDF-S QSO was observed with STIS in G430M at two central wavelengths: 3165 and 3425 Å. The HDF-QSO was also observed with the G230L (cenwave=2376 Å), E230M (cenwave=2707 Å) and G140L (cenwave=1425 Å) gratings. The wavelength calibration was carried out via standard procedures in calstis, using contemporaneous observations of the internal calibration lamp. The spectra obtained with one of the central wavelength settings of G430M overlaps with the deep high-resolution spectra obtained using UCLES at the AAT (Outram et al. 1998), and provides a good opportunity to check the wavelength calibration. Fig 3. shows the overlapping region of the spectra, which shows that the derived wavelengths (after the wavelengths were converted to vacuum) match to better than 1/10 of a pixel, which is same as the accuracy in wavelength determination. A cross correlation of the ground based observations and the STIS spectrum shows that the wavelength discrepancy is less than 1/10 of a pixel. This further confirms our ear-

lier result that there is no significant offset between the internal and external wavelengths for the STIS first order CCD modes.



## 8. The MAMA first-order and Echelle modes

The HDF-S QSO was also observed in the UV wavelengths with the G140L, G230L and E230M gratings. Table 2 gives the details of these observations. For G230L, the wavelength range had a slight overlap with the G430M; comparison of the G230L and G430M wavelengths show excellent agreement (Fig. 4). The Lyman alpha absorption lines observed by UCLES have their corresponding higher order Lyman lines in the E230M and G230L spectra, which were also used to check the internal to external wavelength accuracy (Savaglio et al. 1999). For E230M, the radial velocities of the higher-order Lyman

series lines agree to within 10 km/s with those measured for the Lyman alpha line in the UCLES spectrum. Finally, the wavelengths derived for the E230M observations were compared directly with G430M observations, which also showed excellent agreement. All these results are shown in Fig. 4 where the error-bars are +/- 1-sigma values as derived from the cross-correlation routine. This confirms that, within the accuracy of the observations, there is no offset between the internal and external wavelength calibration for the MAMA first order and Echelle modes.

### ***Acknowledgments***

I would like to thank Tony Keyes for his help in the proposal submission phase, and the HDFS-spectroscopy team, in particular Brian Espey, Sandra Savaglio and Harry Ferguson, for permission to use the results from the cross-correlation of the various STIS data and UCLES data.

### ***References:***

- Bobrowsky, M., Sahu, K.C., Parthasarathy, M., Garcia, P., 1998, Nature, 392, 469
- Outram, P.J. et al. 1998, astro-ph/9809404
- Parthasarathy, M., Sahu, K.C., et al., 1993, Astron. Astrophys. 267, L19
- Waters, R., Sahu, K.C., 1993, Proc. IAU Symp.155 on Planetary Nebulae, p271
- Savaglio, S. et al. 1999, ApJ, submitted for publication, astro-ph/9901022
- Williams, R., 1999, BAAS (in press)
- Woodgate, B. et al. 1998, PASP, 110, 1183